

**HYDROCRACKING AND HYDRODESULPHURIZATION
ACTIVITIES OF NiMo CATALYST SUPPORTED ON
ALUMINA AND ACTIVATED CARBONS FOR
PETROLEUM RESIDUAL OIL**

By

AHMED MUBARAK AHMED ALSOBAAI

**Thesis submitted in fulfillment of the
requirements for the degree of
Master of Science**

September 2003

ACKNOWLEDGMENTS

The work described in this thesis could not have been completed without the assistance of Allah S.W.T. and many people. I wish to express my sincere gratitude to everyone who has made this research possible. I express my deep appreciation to my supervisor, Dr. Bassim H. Hameed for his constant support, encouragement, and advice, which made completion of my study possible. Special thanks to my co-supervisor, Dr. Ridzuan Zakaria for his friendliness and helpfulness through this research work in both, academic and practical sides.

I would also like to thank the Dean of School of Chemical Engineering, Associate Professor Dr. Abdul Rahman Mohamed for the modern facilities available in the laboratories in the school that makes the research go smoothly. I would like to thank all the administrative staff, friends and colleagues in the school for their help. I highly appreciate the cooperation from all the technicians in the laboratories, particularly Mr. Fakharudin, Mohd. Faiza, Shamsul Hidayat, Mohd. Yusuf, Yong and Mrs. Ainun, who have been continuously encouraging and helping me in my research.

I would like to thank School of Materials and Mineral Resources Engineering for the analysis of samples using XRF equipment, and School of Biology for the analysis of samples using SEM equipments.

Finally, I am deeply grateful to my parents, sisters, relatives, friends and my beloved wife for their continued prayers and moral support. Special thanks are due to everyone who has asked the question, "When will you be finished?"

TABLE OF CONTENTS

	Page
TITLE	i
ACKNOWLEDGEMENTS	ii
TABLE OF CONTENTS	iii
LIST OF TABLES	viii
LIST OF FIGURES	xi
LIST OF PLATES	xviii
SYMBOLS AND ABBREVIATIONS	xix
GLOSSARY	xxi
ABSTRAK	xxiv
ABSTRACT	xxvi
CHAPTER 1 INTRODUCTION	1
OBJECTIVES OF THE RESEARCH	4
ORGNIZATION OF THE THESIS	4
CHAPTER 2 LITERATURE SURVEY	6
2.1 PETROLEUM RESIDUAL OIL	6
2.2 HYDROCRACKING AND HYDROTREATING OF RESIDUAL OIL	14
2.2.1 Hydrocracking process	14
2.2.2 Chemical reactions	23

2.2.3 Catalysts	24
(A) Active components	26
(B) Promoters	27
(C) Support	28
2.2.4 Catalyst development	36
(A) Impregnation	36
(B) Calcination	36
(C) Pretreatments	37
2.2.5 Characterization of catalysts	39
(A) Surface properties	39
(B) Scanning electron microscopy (SEM)	40
(C) Surface acidity	41
(D) Composition of catalysts	41
2.3 STATISTICAL ANALYSIS	42
CHAPTER 3 EXPERIMENTAL	44
3.1 INTRODUCTION	44
3.2 MATERIALS	44
3.2.1 Sample of petroleum residual oil	44
3.2.2 Chemicals	47
3.2.3 Gases	47
3.2.4 Catalysts	47
(A) NiMo/Al ₂ O ₃ catalyst	47
(B) Prepared NiMo/activated carbon catalysts	49
(C) Synthesized catalysts	50

3.3 GENERAL DESCRIPTION OF EQUIPMENT	52
3.3.1 Activated carbon preparation system	52
3.3.2 Catalyst pretreatment system	54
3.3.3 Hydrocracking reaction system	57
3.3.4 Analysis system	61
3.3.4.a Viscosity test	61
3.3.4.b Elemental analysis	63
3.3.4.c ASTM distillation analysis	65
3.3.4.d Gas chromatograph (GC)	68
3.3.5 Characterization of catalysts	68
3.3.5.a Nitrogen adsorption	68
3.3.5.b Elemental composition measurements	69
3.3.5.c Scanning electron microscopy (SEM)	71
3.3.5.d Temperature-programmed desorption (TPD)	71
3.3.5.e Thermogravimetric analyzer (TGA)	73
3.4 EXPERIMENTAL PROCEDURES	73
3.4.1 Activated carbon preparation	73
3.4.2 Catalysts pretreatments	75
(A) Presulfidation	75
(B) Reduction	75
3.4.3 Procedure of hydrocracking reaction	77
3.5 SAFETY PRECAUTIONS	77
CHAPTER 4 RESULTS AND DISCUSSION	78
4.1 INTRODUCTION	78

4.2 EFFECT OF OPERATING CONDITIONS ON CATALYTIC HYDROCRACKING OF PETROEUM RESIDUAL OIL	82
4.2.1 Product distributions	82
4.2.2 Hydrodesulphurization (HDS), hydrodenitrogenation (HDN) and H/C atomic ratio	90
4.3 DESIGN OF EXPERIMENTS	98
4.4 FINDING SUITED OPERATING CONDITIONS	122
4.5 CHARACTRIZATION OF CATALYSTS	128
4.5.1 Nitrogen adsorption measurements	128
4.5.2 Scanning electron microscopy (SEM)	128
4.5.3 X-ray fluorescence (XRF)	132
4.5.4 Temperature –programmed desorption (TPD) acidity measurements	132
4.5.5 Thermal gravity analyzer (TGA)	135
4.6 ANALYSIS OF PRODUCTS	138
4.6.1 Liquid products	138
4.6.1.a ASTM distillation	138
4.6.1.b Elemental analyzer	138
4.6.1.c Viscosity tests	138
4.6.2 Gaseous products	141
4.6.3 Coke	141
4.7 CATALYTIC HYDROCRACKING OF PETROLEUM RESIDUAL OIL OVER DIFFERENT TYPES OF CARBON-BASED CATALYSTS	146
4.7.1 Product distributions	146
4.7.2 Hydrodesulphurization (HDS), hydrodenitrogenation (HDN) and H/C atomic ratio	149
4.8 PERFORMANCE OF PRETREATED NiMo/AC1 CATALYST	152

4.8.1 Product distributions	152
4.8.2 Hydrodesulphurization (HDS), hydrodenitrogenation (HDN) and H/C atomic ratio	154
3.9 REACTION MECHANISM	156
CHAPTER 5 CONCLUSIONS	158
CHAPTER 6 RECOMMENDATIONS	160
APPENDIX A	161
REFERENCES	172

LIST OF TABLES

	<u>Page</u>	
Table 2.1	Properties of typical atmospheric residual oil (>340°C)	9
Table 2.2	Properties of typical vacuum residual oil (>560 °C)	10
Table 2.3	Typical elemental composition and H/C atomic ratio of typical petroleum residual oil	11
Table 2.4	Chemical composition of petroleum residual oil	12
Table 2.5	Summary of conventional and improved catalysts for residue conversion and low-sulphur fuel oil production	25
Table 3.1	Elemental composition analysis, wt % of the residual oil	45
Table 3.2	Distillation analysis of the residual oil	45
Table 3.3	Viscosity of the residual oil at 50 °C	45
Table 3.4	Chemical composition and physical properties of the NiMo/Al ₂ O ₃ catalyst	48
Table 3.5	Physical properties of activated carbons used in this work	50
Table 3.6	Products distribution	66
Table 4.1	Effect of operating conditions on total conversion and product distributions for catalytic hydrocracking of atmospheric petroleum residual oil over commercial NiMo/Al ₂ O ₃ catalyst	83
Table 4.2	Effect of operating conditions yield of distillate fuels for catalytic hydrocracking of petroleum residual oil over commercial NiMo/Al ₂ O ₃ catalyst	84

	<u>Page</u>	
Table 4.3	Effect of operating conditions on HDS, HDN and H/C for catalytic hydrocracking of atmospheric petroleum residual oil over commercial NiMo/Al ₂ O ₃ catalyst	91
Table 4.4	The three factors, temperature, time, catalyst ratio and their level	99
Table 4.5	Design layout with coded factor levels	101
Table 4.6	The experimental results obtained according to the central composite design	102
Table 4.7	Sequential model sum of squares for conversion	103
Table 4.8	Sequential model sum of squares for gasoline yield	103
Table 4.9	Sequential model sum of squares for HDS activity	103
Table 4.10	Lack of fit tests for conversion	105
Table 4.11	Lack of fit tests for gasoline yield	105
Table 4.12	Lack of fit tests for HDS activity	105
Table 4.13	Model summary statistics of conversion	106
Table 4.14	Model summary statistics of gasoline yield	106
Table 4.15	Model summary statistics of HDS activity	106
Table 4.16	Analyses of variance (ANOVA) for conversion	107
Table 4.17	Analyses of variance (ANOVA) for gasoline yield	107
Table 4.18	Analyses of variance (ANOVA) for HDS activity	108
Table 4.19	The results of the R-squared values for conversion, gasoline yield and HDS activity responses	110
Table 4.20	Coefficients of the linear model for conversion response	110

	<u>Page</u>	
Table 4.21	Coefficients of the linear model for gasoline yield response	111
Table 4.22	Coefficients of the quadratic model for HDS activity response	111
Table 4.23	Actual and predicted values for conversion obtained from linear model	114
Table 4.24	Actual and predicted values for gasoline yield obtained from linear model	114
Table 4.25	Actual and predicted values for HDS activity obtained from quadratic model	115
Table 4.26	The design status for the three responses	123
Table 4.27	Selected values obtained from response surface methodology	123
Table 4.28	BET surface area, pore volume and average pore diameter of supports and catalysts measured by N ₂ adsorption	129
Table 4.29	Viscosity of liquid products obtained at ambient temperature	140

LIST OF FIGURES

	<u>Page</u>
Figure 2.1 Schematic diagram of refinery distillation	7
Figure 2.2 HDS activity of dispersed and presulphided supported catalyst (Tian <i>et al.</i> , 1998)	18
Figure 2.3 HDN activity of dispersed and presulphided supported catalyst Tian <i>et al.</i> , 1998)	18
Figure 2.4 Proposed reaction mechanism for the effect of H ₂ S on HDS reactions (Farag <i>et al.</i> , 2003)	22
Figure 2.5 SEM images of wood based activated carbons; magnification is 450:1	33
Figure 2.6 SEM images of peat based activated carbons; magnification is 1000:1	33
Figure 2.7 SEM images of coconut shell based activated carbons; magnification is 1000:1	34
Figure3.1 Schematic diagram of activated carbon-based catalyst preparation steps	51
Figure 3.2 Schematic diagram of catalyst pretreatment system	55
Figure 3.3 Schematic diagram of experimental set up for hydrocracking of residual oil	58
Figure 3.4 Schematic diagram for the analyses of various products from hydrocracking of residual oil and catalyst characterizations	62
Figure 3.5 Schematic diagram of the activated carbon preparation	75
Figure 4.1 Effect of different operating conditions on total conversion, liquid, gas and coke products over commercial NiMo/Al ₂ O ₃ catalyst	85
Figure 4.2 Effect of different operating conditions on yield of distillate fuels over commercial NiMo/Al ₂ O ₃ catalyst	85

	<u>Page</u>	
Figure 4.3	Effect of temperature on total conversion, liquid, gas and coke products over commercial NiMo/Al ₂ O ₃ catalyst at constant time of 160 min and catalyst ratio of 0.80	87
Figure 4.4	Effect of temperature on yield of distillate fuels over commercial NiMo/Al ₂ O ₃ catalyst at constant time of 160 min and catalyst ratio of 0.80	87
Figure 4.5	Effect of time on total conversion, liquid, gas and coke products over NiMo/Al ₂ O ₃ catalyst at constant temperature of 300 °C and catalyst ratio of 0.80	89
Figure 4.6	Effect of time on yield of distillate fuels over NiMo/Al ₂ O ₃ catalyst at constant temperature of 300 °C and catalyst ratio of 0.80	89
Figure 4.7	Effect of catalyst ratio on total conversion, liquid, gas and coke products over commercial NiMo/Al ₂ O ₃ catalyst at constant temperature of 300 °C and time of 160 min	91
Figure 4.8	Effect of catalyst ratio on yield of distillate fuels over commercial NiMo/Al ₂ O ₃ catalyst at constant temperature of 300°C and time of 160 min	91
Figure 4.9	Effect of different operating conditions on HDS, HDN and increment of H/C over commercial NiMo/Al ₂ O ₃ catalyst	93
Figure 4.10	Effect of temperature on HDS, HDN and increment of H/C over commercial NiMo/Al ₂ O ₃ catalyst at constant time of 160 min and catalyst ratio of 0.80	96
Figure 4.11	Effect of time on HDS, HDN and increment of H/C over commercial NiMo/Al ₂ O ₃ catalyst at constant temperature of 300 °C and catalyst ratio of 0.80	96

	<u>Page</u>	
Figure 4.12	Effect of catalyst ratio on HDS, HDN and increment of H/C over commercial NiMo/Al ₂ O ₃ catalyst at constant temperature of 300°C and time of 160 min	97
Figure 4.13	The three factors layout for the central composite design (CCD)	99
Figure 4.14	Normal probability plot of the residuals for conversion	116
Figure 4.15	Normal probability plot of the residuals for gasoline yield	116
Figure 4.16	Normal probability plot of the residuals for HDS activity	117
Figure 4.17	Contour and response surface plots of conversion as a function of temperature and time at the mid-level slice of the catalyst ratio	117
Figure 4.18	Contour and response surface plots of conversion as a function of catalyst ratio and time at the mid-level slice of the temperature	118
Figure 4.19	Contour and response surface plots of conversion as a function of catalyst ratio and temperature at the mid-level slice of the time	118
Figure 4.20	Contour and response surface plots of gasoline yield as a function of temperature and time at the mid-level slice of the catalyst ratio	119
Figure 4.21	Contour and response surface plots of gasoline yield as a function of catalyst ratio and time at the mid-level slice of the temperature	119
Figure 4.22	Contour and response surface plots of gasoline yield as a function of catalyst ratio and temperature at the mid-level slice of the time	120
Figure 4.23	Contour and response surface plots of HDS activity as a function of temperature and time at the mid-level slice of the catalyst ratio	120
Figure 4.24	Contour and response surface plots of HDS activity as a function of catalyst ratio and time at the mid-level slice of the temperature	121

	<u>Page</u>	
Figure 4.25	Contour and response surface plots of HDS activity as a function of catalyst ratio and temperature at the mid-level slice of the time	121
Figure 4.26	Ramps report on numerical study	124
Figure 4.27	Desirability histogram for selected solution	124
Figure 4.28	Contour and response surface plots of desirability as a function of temperature and time at the constant value of the catalyst ratio	125
Figure 4.29	Contour and response surface plots of desirability as a function of catalyst ratio and time at the constant value of the temperature	126
Figure 4.30	Contour and response surface plots of desirability as a function of catalyst ratio and temperature at the constant value of the time	127
Figure 4.31	Pore size distributions of different catalysts used in this study	130
Figure 4.32	SEM photographs for AC1 support	131
Figure 4.33	SEM photographs for NiMo/AC1 catalyst	131
Figure 4.34	XRF spectra for NiMo/AC1 catalyst: (a) Nickel, (b) Molybdenum	133
Figure 4.35	TPD acidity for different catalysts used in this study	134
Figure 4.36	TGA result for prepared NiMo/AC1 catalyst	135
Figure 4.37	TGA result for prepared NiMo/AC2 catalyst	136
Figure 4.38	TGA result for prepared NiMo/AC3 catalyst	136
Figure 4.39	TGA result for prepared NiMo/AC4 catalyst	137
Figure 4.40	TGA result for prepared NiMo/AC5 catalyst	137
Figure 4.41	Gaseous product analysis of catalytic hydrocracking of residual oil over NiMo/AC1 catalyst at 330°C, 200 minutes and 1.1 of catalyst ratio	142

	<u>Page</u>
Figure 4.42 TGA analysis for coke produced from cracking of residual oil over commercial NiMo/Al ₂ O ₃ at temperature of 330 °C , time of 200	143
Figure 4.43 TGA analysis for coke produced from cracking of residual oil over NiMo/AC1 at temperature of 330 °C , time of 200 minutes and catalyst ratio of 1.1	143
Figure 4.44 TGA analysis for coke produced from cracking of residual oil over NiMo/AC2 at temperature of 330 °C , time of 200 minutes and catalyst ratio of 1.1	144
Figure 4.45 TGA analysis for coke produced from cracking of residual oil over NiMo/AC3 at temperature of 330 °C , time of 200 minutes and catalyst ratio of 1.1	144
Figure 4.46 TGA analysis for coke produced from cracking of residual oil over NiMo/AC4 at temperature of 330 °C , time of 200 minutes and catalyst ratio of 1.1	145
Figure 4.47 TGA analysis for coke produced from cracking of residual oil over NiMo/AC5 at temperature of 330 °C, time of 200 minutes and catalyst ratio of 1.1	145
Figure 4.48 Effect of catalyst types on total conversion, liquid, gas and coke products for catalytic hydrocracking of petroleum residual oil at selected operating conditions	147
Figure 4.49 Effect of catalyst types on yield of distillate fuels for catalytic hydrocracking of petroleum residual oil at selected operating conditions	148

	<u>Page</u>	
Figure 4.50	Effect of catalyst types on HDS, HDN and H/C for catalytic hydrocracking of petroleum residual oil at selected operating conditions	150
Figure 4.51	Effect of catalyst pretreatments on total conversion, liquid, gas and coke for catalytic hydrocracking of petroleum residual oil at selected operating conditions	152
Figure 4.52	Effect of catalyst pretreatments on yield of distillate fuels for catalytic hydrocracking of petroleum residual oil at selected operating conditions	152
Figure 4.53	Effect of catalyst pretreatments on HDS, HDN and H/C for catalytic hydrocracking of petroleum residual oil at selected operating conditions	155
Figure 4.54	Schematic diagram of reaction mechanism pathway for catalytic hydrocracking of petroleum residual oil	157
Figure A.1	Actual and predicted plot for conversion	161
Figure A.2	Actual and predicted plot for gasoline yield	162
Figure A.3	Actual and predicted plot for HDS activity	162
Figure A.4	Contour and response surface plots of conversion as a function of temperature and time at the constant value of the catalyst ratio	163
Figure A.5	Contour and response surface plots of conversion as a function of catalyst ratio and time at the constant value of the temperature	164
Figure A.6	Contour and response surface plots of conversion as a function of catalyst ratio and temperature at the constant value of the time	165

		<u>Page</u>
Figure A.7	Contour and response surface plots of gasoline yield as a function of temperature and time at the constant value of the catalyst ratio	166
Figure A.8	Contour and response surface plots of gasoline yield as a function of catalyst ratio and time at the constant value of the temperature	167
Figure A.9	Contour and response surface plots of gasoline yield as a function of catalyst ratio and temperature at the constant value of the time	168
Figure A.10	Contour and response surface plots of HDS activity as a function of temperature and time at the constant value of the catalyst ratio	169
Figure A.11	Contour and response surface plots of HDS activity as a function of catalyst ratio and time at the constant value of the temperature	170
Figure A.12	Contour and response surface plots of HDS activity as a function of catalyst ratio and temperature at the constant value of the time	171

LIST OF PLATES

		<u>Page</u>
Plate 3.1	Atmospheric petroleum residual oil	46
Plate 3.2	Photograph of the equipment set up for the preparation of activated carbon	53
Plate 3.3	Photograph of the tubular reactor used for catalyst pretreatment	56
Plate 3.4	Photograph of the experimental set up for hydrocracking of residual oil	59
Plate 3.5	Photograph of the high-pressure batch reactor	60
Plate 3.6	Photograph of viscometer instrument	64
Plate 3.7	Photograph of elemental analyzer instrument	65
Plate 3.8	Photograph of ASTM distillation unit	67
Plate 3.9	Photograph of Autosorb 1 instrument	70
Plate 3.10	Photograph of TPD instrument	72
Plate 3.11	Photograph of the thermogravimetric analyzer instrument	74

SYMBOLS AND ABBREVIATIONS

<u>Symbol</u>	<u>Description</u>	<u>unit</u>
2FI	Two Factor Interaction	-
AC	Activated Carbon	-
ANOVA	Analyses of Variance	-
API	American Petroleum Institute	o
ASTM	American Society for Testing Materials	-
BET	Brunauer-Emmett-Teller	m ² /g
CI	Confidence Interval	-
C.V	Coefficient of Variation	-
CCD	Central Composite Design	-
DBT	Dibenzothiophene	-
DF	Degree of Freedom	-
DOE	Design of Experiment	-
EA	Elemental Analyzer	-
ED	Ethyldecanoate	-
FCC	Fluid Catalytic Cracking	-
FID	Flame Ionization Detector	-
GC	Gas Chromatograph	-
GHSV	Gas Hourly Space Velocities	h ⁻¹
H/C	Hydrogen/Carbon	-
HDN	Hydrodenitrogenation	-

HDS	Hydrodesulphurization	-
HVGO	Heavy Vacuum Gas Oil	-
IUPAC	International Union of Pure and Applied Chemistry	-
MA	Methylacetone	-
n. a	not applicable	-
PRESS	Prediction Error Sum of Squares	-
Prob	Probability	-
RSM	Response Surface Methodology	-
SEM	Scanning Electron Microscopy	-
Std. Dev	Standard Deviation	-
STP	Standard Temperature and Pressure	-
TGA	Thermal Gravimetric Analysis	-
TPD	Temperature Programmed Desorption	-
WHSV	Weight Hourly Space Velocities	h ⁻¹
XRF	X-ray Fluorescence	-

GLOSSARY

95% Confidence Interval High and Low:	These two columns represent the range that the true coefficient should be found in 95% of the time. If this range spans 0 (one limit is positive and the other negative) then the coefficient of 0 could be true, indicating the factor has no effect.
Adequate Precision:	Adequate precision is a measure of the range in predicted response relative to its associated error, in other words a signal to noise ratio. Its desired value is 4 or more.
Adjusted R Square:	Adjusted R-Squared represents the amount of variation that can be explained by the model. This is the R-Squared value after adjusting for the number of terms in the model relative to the number of design points.
Aliased Models:	Not enough experiments have been run to independently estimate all the terms for this model.
Alpha (α):	In a central composite design (CCD), it represents the distance from the centre of the design space to a star (or axial) point. In a power transformation, alpha is related to the power, lambda as being equal to one minus lambda.
Central Composite Design:	<p>The most popular response surface method (RSM) design is the central composite design (CCD). A CCD has three groups of design points:</p> <ul style="list-style-type: none">(a) two-level factorial or fractional factorial design points(b) axial points (sometimes called "star" points)(c) centre points <p>CCD is designed to estimate the coefficients of a quadratic model. All point descriptions will be in terms of coded values of the factors.</p>
Centre points:	Experimental runs with all numerical factor levels set at the midpoint of their high and low settings. They are used to test curvature and, if replicated, as a test for lack of fit.
Coefficient of Variation:	The coefficient of variation is a measure of residual variation of the data relative to the size of the mean. It is the standard deviation divided by the dependent mean and expressed as a percent.
Corrected Total:	This is totals of all information corrected for the mean.
Degree of Freedom:	The number of independent comparisons available to estimate a parameter. Usually the number of model parameters is minus one.
Design Space:	An imaginary area bounded by the extremes of the tested factors.

F Probability:	This is the probability associated with adding the additional terms to the model. The highest order model (that is not aliased) in which the additional terms are significant should be usually chosen.
F Value:	The F distribution is a probability distribution used to compare variances by examining their ratio. If they are equal then the F value would equal 1. The F value in the ANOVA table is the ratio of model mean square (MS) to the appropriate error mean square. The larger the ratio, the larger the F value and the more likely that the variance contributed by the model is significantly larger than random error.
Lack of Fit:	This is the variation of the data around the fitted model. If the model does not fit the data well, this will be significant.
Mean Square:	The sum of squares divided by the number of degrees of freedom (SS/DF). This is used to calculate the F-value for the models.
Model:	The model is the empirical mathematical model that is fit to the data. Polynomial models are used in Design-Expert. In the ANOVA the model term is the source of variation accounted for by the model terms.
Predicted R Square:	It represents the amount of variation in new data explained by the model. A negative Predicted R-Squared means that the overall mean is a better predictor than this model.
Prediction Error Sum of Squares:	A measure of how a particular model fits each design point. The coefficients for any model are calculated without the first design point. The model is used to predict the first point and then the new residual is calculated for this point. This is done for each data point and then the squared residuals are summed.
Pure Error:	Experimental error, or pure error, is the normal variation in the response which appears when an experiment is repeated. Repeated experiments rarely produce exactly the same results. Pure error is the minimum variation expected in a series of experiments. It can be estimated by replicating points in the design. The more replicated points the better will be the estimate of the pure error. Pure error is used to test the lack of fit terms for possible significance.
R Square:	R-Squared is the correlation coefficient for the model. It should be close to one.
Residual:	Consists of terms used to estimate experimental error.
Response:	A measurable product or process characteristic thought to be affected by the experimental factors.

- Standard Deviation:** This estimates the standard deviation of the error in the design. It is sometimes referred to as the Root Mean Square Error. It should be relatively small.
- Sum of Square:** The sum of the squared distances from the mean due to an effect.
- Term Coefficient:** This is the model coefficient or parameter for this particular term. Since this value is expressed in coded units, it can compare its relative magnitude to other term coefficients to estimate relative effect.

AKTIVITI-AKTIVITI PENGHIDROPECAHAN DAN PENGHIDRONYAHSULFURAN MANGKIN NiMo YANG DISOKONG OLEH ALUMINA DAN KARBON-KARBON TERAKTIF UNTUK MINYAK SISA PETROLEUM

ABSTRAK

Kajian ini bertujuan untuk mempertingkatkan kualiti minyak sisa petroleum dengan cara menukarkannya kepada produk-produk yang lebih ringan menggunakan beberapa jenis mangkin yang berlainan. Proses ini dilakukan secara kelompok di bawah pelbagai keadaan operasi; dalam suhu julat 250-350 °C, masa tindakbalas 90-230 min dan nisbah mangkin 0.3-1.30 menggunakan reaktor teraduk bertekanan tinggi dengan kehadiran hidrogen dan mangkin.

Sebagai permulaan, mangkin komersil NiMo/Al₂O₃ telah digunakan untuk mencari keadaan-keadaan operasi julat bagi pemecahan hidro bermangkin minyak sisa petroleum. Rekabentuk eksperimen, (DOE), digunakan untuk mendapatkan keadaan-keadaan operasi yang julat. Didapati bahawa keadaan-keadaan operasi yang julat bagi penghidropecahan bermangkin bagi minyak sisa petroleum oleh mangkin NiMo/Al₂O₃ bersulfida komersial ialah suhu 330 °C, masa 200 min dan nisbah mangkin 1.1.

Penghidropecahan minyak sisa petroleum juga telah dijalankan menggunakan mangkin nikel molibdenum/karbon teraktif (NiMo/AC) dengan pelbagai jenis karbon teraktif (AC1, AC2, AC3, AC4 dan AC5) yang dioperasikan pada keadaan operasi yang dipilih seperti yang diperolehi melalui tindakbalas menggunakan mangkin NiMo/Al₂O₃ komersil. Aktiviti-aktiviti penghidronyhsulfuran dan penghidronyahnitrogenan juga dikaji semasa tindakbalas tersebut. Didapati bahawa mangkin NiMo/AC1 memberikan

penukaran dan produk tersuling yang paling tinggi. Penukaran dan bahan api tersuling keseluruhan ialah masing-masing 10 dan 15 % berat lebih tinggi daripada mangkin NiMo/Al₂O₃ komersil. Mangkin NiMo/AC1 juga menunjukkan aktiviti-aktiviti penghidronyahsulfuran, penghidronyahnitrogenan serta nisbah atom H/C yang paling tinggi. Ia memberikan masing-masing 41.33, 24.32 dan 36.55 % berat bagi penghidronyahsulfuran, penghidronyahnitrogenan dan nisbah atom H/C. Sementara itu, mangkin NiMo/Al₂O₃ komersial memberikan masing-masing 37.33, 22.52 dan 12.7 % berat bagi penghidronyahsulfuran, penghidronyahnitrogenan dan nisbah atom H/C. Mangkin berasaskan karbon teraktif yang lain menunjukkan aktiviti yang hampir sama dengan mangkin NiMo/Al₂O₃ komersil.

Beberapa proses pra-pengolahan yang berbeza telah digunakan ke atas mangkin NiMo/AC1 sebelum ujian aktiviti. Proses-proses ini ialah pensulfidaan dan penurunan. Keputusan menunjukkan mangkin tersulfida memberikan aktiviti pemecahan hidro yang lebih tinggi berbanding mangkin terturun. Ia memberikan masing-masing 76.92, 14.09, 4.55, 11.22, 14.79 dan 44.65 % berat bagi penukaran keseluruhan, hasil gasolin, kerosin, bahan api jet, diesel dan bahan api tersuling keseluruhan. Sebagai tambahan, ia juga memberikan aktiviti-aktiviti penghidronyahsulfuran dan penghidronyahnitrogenan yang lebih tinggi berbanding mangkin terturun dengan masing-masing 41.33 dan 24.32 % berat.

Beberapa analisis yang berlainan telah dilakukan untuk menentukan komposisi suapan dan produk-produk pemecahan hidro serta untuk tujuan pencirian mangkin. Analisis-
analisis ini termasuklah penyerapan nitrogen, X-ray floresens (XRF), mikroskop elektron (SEM), penyahjerapan berprogramkan suhu (TPD), analisis termogravimetri (TGA), penyulingan *American society for testing of materials* (ASTM), analisis unsur (EA), kromatografi gas dan meter likat.

ABSTRACT

This study aims to improve petroleum residual oil quality by converting it into lighter products over different types of catalysts. The process was conducted in a batch mode under various operating conditions, temperature in range 250-350 °C, reaction time 90-230 min and catalyst ratio 0.3-1.30 using a high-pressure stirred reactor in the presence of hydrogen and catalyst.

At first commercial NiMo/Al₂O₃ catalyst was used to find the range of operation conditions for catalytic hydrocracking of petroleum residual oil. Statistical design of experiment, (DOE), was used to obtain the range of operating conditions. It was found that the range of operating conditions for catalytic hydrocracking of petroleum residual oil over commercial NiMo/Al₂O₃ sulphided catalyst are: temperature of 330 °C, time of 200 min and catalyst ratio of 1.1.

The hydrocracking of petroleum residual oil was also conducted over synthesized Nickel-Molybdenum/Activated carbon (NiMo/AC) catalysts with various types of activated carbons (AC1, AC2, AC3, AC4 and AC5) operated at the selected operating conditions obtained from the reaction with commercial NiMo/Al₂O₃ catalyst. Hydrodesulphurization and hydrodenitrogenation activities were also examined during the reaction process. It was found that NiMo/AC1 catalyst had the highest conversion and distillate products. The conversion and total distillate fuels were 10 and 15wt%, respectively higher than commercial NiMo/Al₂O₃ catalyst. NiMo/AC1 catalyst also showed highest HDS, HDN activities and H/C atomic ratio. It gave 41.33, 24.32 and 36.55 wt% of HDS, HDN and H/C atomic ratio, respectively. While commercial

NiMo/Al₂O₃ gave 37.33, 22.52 and 12.7 wt% of HDS, HDN and H/C atomic ratio, respectively. Other activated carbon-based catalysts showed activity near that of commercial NiMo/Al₂O₃ catalyst.

Different pretreatments were used for NiMo/AC1 catalyst before activity tests. These are sulphidation and reduction. The results showed that sulphided catalyst gave higher hydrocracking activity than reduced catalyst. It gave 76.92, 14.09, 4.55, 11.22, 14.79 and 44.65 wt% total conversion, yields of gasoline, kerosene, jet fuel, diesel and total distillate fuels, respectively. Furthermore, it gave higher activity of HDS and HDN than reduced catalyst. It gave 41.33 and 24.32 wt% of HDS and HDN activities, respectively.

Different analyses were carried out to determine the composition of feed and products of hydrocracking and to characterize catalysts. These analyses include: nitrogen adsorption, X-ray fluorescence (XRF), scanning electron microscopy (SEM), temperature programmed desorption (TPD), thermogravimetric analyzer (TGA), American society for testing materials (ASTM) distillation, elemental analyzer (EA), gas chromatography (GC) and viscometer.

CHAPTER ONE
INTRODUCTION

CHAPTER ONE

INTRODUCTION

The demand for energy is still increasing to provide electricity to megalopolis, and fuels for transportation. The main primary energy in the world is fossil fuels (crude oil, natural gas and coal). Coal only provides enough reserves for several countries, but it poses important environmental problems; it is largest source of carbon dioxide emissions which will be constantly increasing. Total crude oil demand is projected to grow and the proven reserves in the world are limited. In the many parts of the world, light oil production is declining and heavy oil conversion, therefore, becomes increasingly important to maintain economic viability of these regions. Many conventional crude oils usually contain 10-30 % residual oil, and the need to process it is very important because of limited fossil fuel resources. Furthermore, crude oils become more expensive and the majority of machines and equipment being made at present are designed to run using liquid fuel.

Since the early 1980s, the demand for heavy oils fuels from petroleum has decreased steadily. The rises of demand for the light fuels particularly gasoline are important to extract much useful materials from crude oil. About 94 % of the projected growth in petroleum consumption stems from increased consumption of light products,

including gasoline, diesel, kerosene, jet fuel, and liquefied petroleum gas, which are more difficult and costly to produce than heavy products. Refined product prices are expected to increase and determined by crude oil costs, refining process costs, marketing costs, and taxes.

Recently, the number of gasoline powered vehicles increased dramatically and the demand for gasoline grew accordingly. Gasoline can be obtained by distillation processes of crude oil or by thermal treatment processes of heavy products as residual oil. Distillation processes produced only a certain amount of gasoline from crude oil.

The thermal cracking process which subjected heavy fuels to both pressure and intense heat is physically breaking the large molecules into smaller ones to produce additional gasoline and distillate fuels. Higher-compression gasoline engines required higher-octane gasoline with better antiknock characteristics. The introduction of catalytic cracking and polymerization processes in the mid- to late 1930s met the demand by providing improved gasoline yields and higher octane numbers.

Various treatment methods have been used to remove nonhydrocarbons, impurities, and other constituents that adversely affect the properties of finished products or reduce the efficiency of the conversion processes. After distillation of crude oil, most of the heterogeneous compounds particularly sulphur compounds remain in the residue, and during thermal treatment of residue the carbon-carbon bonds are cleaved, therefore hydrogen is needed to prevent formation of coke. Various processes improved gasoline quality and yield and produced higher-quality products. Some of these involved the use of catalysts and hydrogen to change molecules and remove sulphur. The more commonly used treating process is hydrotreating (hydrodesulphurization and hydrodenitrogenation).

Hydrodesulphurization (HDS) and hydrodenitrogenation (HDN) are a catalytic cracking which use hydrogen at high pressure and temperature in the presence a catalyst to reduce sulphur and nitrogen, and to produce lighter oils by cracking the heavy oil molecules. Many catalysts are used for the hydrotreating process are formed by composting various transition metals with the solid support such as alumina, silica, alumina-silica, magnesia and zeolites. Nickel and molybdenum are two of the more common metals that are used as hydrotreating catalysts and other metals may be used such as a combination of cobalt and molybdenum and nickel tungsten.

The used of activated carbons as a catalyst support offers some advantages over the more traditional oxide carries, such as possess a high surface area with controlled pore volume and pore size. Activated carbons have important contributions from the micropores, mesopores and macropores and therefore are considered to be reliable in many applications. Such advantages make it an attractive catalyst support. It is inexpensive and can be prepared from agricultural by-products and wastes. A very important point for the economic use of precious metal catalysts, especially high loaded ones, is recovery, refining and recycling of the metal. This procedure is simplified by the use of activated carbon as support, for this material can be burnt off, leading to highly concentrated ashes that permit an economical recovery of the precious metal.

This research concentrated on the activated carbon as a support for NiMo catalyst in order to investigate its performance for hydrocracking of residual oil and comparing its activity with that of commercial NiMo/Al₂O₃ catalyst

OBJECTIVES OF THE RESEARCH

The main objectives of this study are:

- 1- To study the effects of important variables (temperature, time and catalyst ratio) in the catalytic hydrocracking of petroleum residual oil using commercial nickel-molybdenum/alumina (NiMo/Al₂O₃) catalyst. The range of operating conditions were obtained using statistical design of experiment (DOE).
- 2- To synthesized a series of nickel-molybdenum/activated carbons catalyst (NiMo/AC) with different types of activated carbons and test the performance of these catalysts at the selected operating conditions.
- 3- To characterize a series of NiMo/activated carbons catalysts in terms of surface area, pore size distribution, thermal stability, acidity strength and morphology.
- 4- To compare the performance of the synthesized catalysts with that of commercial catalyst.

ORGANIZATION OF THE THESIS

There are six chapters in the thesis, and each chapter give valuable information of the thesis.

Chapter two presents a review of literature. It is divided into three sections, the first section presents a general background on petroleum residual oil and its chemical

composition, the second section gives details aspects of hydrocracking and hydrotreating processes, and the last section gives a discussion of statistical analysis.

Chapter three deals with experimental methodology and focuses on the various methods used in this study. This chapter describes the materials and the experimental apparatus used in this work. The apparatus comprised four parts, i.e. the catalyst pretreatment system, the hydrocracking system, product analysis and characterization of catalysts. It describes as well the experimental procedures and safety precautions adopted.

Chapter four presents the experimental results together with the discussion. It is divided into nine sections; the first section gives general introduction on this chapter, the second section presents the effects of operating conditions on catalytic hydrocracking of petroleum residual oil, the third section gives details on statistical design of experiment, the fourth section presents selection of operating conditions, the fifth section presents characterization studies of catalysts and supports, the sixth sections gives the analyses of liquid, gas and solid products, the seventh section presents results and discussions of catalytic hydrocracking of petroleum residual oil over different types of carbon-based catalysts, the eighth section gives results and discussions of catalytic hydrocracking of petroleum residual oil using different catalyst pretreatments, the last section gives the proposal reaction mechanism.

Chapter five gives conclusions of this work. Finally, Chapter six gives recommendations for future studies.

CHAPTER TWO
LITERATURE SURVEY

CHAPTER TWO

LITERATURE SURVEY

2.1 PETROLEUM RESIDUAL OIL

Petroleum is a very complex mixture containing many different hydrocarbon compounds like paraffin, naphthene and aromatic hydrocarbons that vary in appearance and composition from one oil field to another. On average, petroleum contains about 84% carbon, 14% hydrogen, 1-3% sulphur and less than 1% each of nitrogen, oxygen, metals and salts. The majority products of petroleum are LPG (liquid petroleum gas), gasoline, kerosene and diesel. These products are separated by distillation in refinery, and in the bottom of distillation columns, residual oil is remained (Gray, 1994; Speight, 1998). Distillation is the separation of crude oil in atmospheric and vacuum distillation columns into groups of hydrocarbon compounds of different boiling point ranges called fractions or cuts. Figure 2.1 shows schematic diagram of petroleum refinery distillation columns (Speight, 1998).

Residual oil is the fraction of crude oil, which is obtained by atmospheric or vacuum distillation of crude oil, and the temperature of the distillation is usually maintained below 350 °C. Petroleum usually contains about 10-30 % residual oil (Gray, 1994).

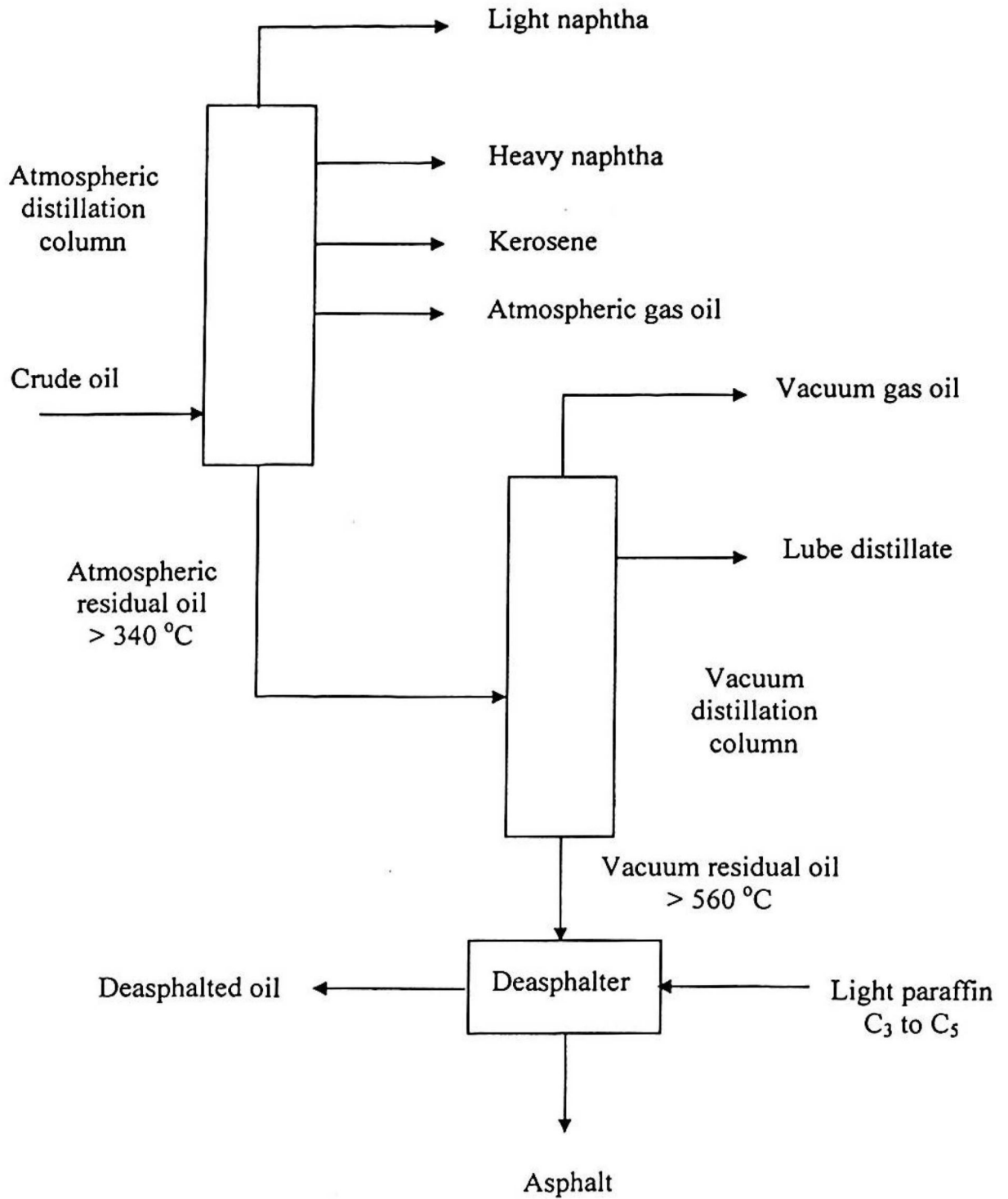


Figure 2.1 Schematic diagram of refinery distillation (Speight, 1998)

Residue has black colour and high viscosity, they maybe liquid at room temperature (generally atmospheric residue) or almost solid (generally vacuum residue) depending upon the nature of the crude oil. Residue consists of a mixture hydrocarbon homogeneous compounds which contain carbon and hydrogen, further hydrocarbon heterogeneous compounds which contain sulphur (for example hydrogen sulphide and methyl mercaptan), nitrogen (i.e andole and carbazole) and oxygen (i.e. methyl alcohol and acetic acid) as well as there are very small amounts of nonhydrocarbon metallic compounds as iron, copper, nickel and vanadium (Speight, 1981). Representative properties of atmospheric and vacuum residual oil are shown in Tables 2.1 and 2.2, respectively (Kabe *et. al.*, 1999).

The composition of petroleum residual oil can vary with the age and location of the crude oil and also the severity of the distillation process. The atomic ratio of hydrogen to carbon gives an indication of heating value and composition properties. This ratio varies little between residues. The typical elemental composition and H/C atomic ratio of typical residual oil may fall within the limits showing in Table 2.3 (Gray, 1994; Kabe *et. al.*, 1999).

The chemical composition of petroleum residual oil depends on the both the original oil and subsequent processing. Some crudes give a residues with a high wax content which corresponds to long chain paraffins and refinery processing give residues with different properties. The main building blocks which are combined to give high boiling point compounds found in residues are shown in Table 2.4 (Gray, 1994).

Petroleum residual oil is often solid or semisolid at room temperature with viscosity and density more than 10^5 mpa.s and 10^3 kg/m³, respectively.

Table 2.1 Properties of typical atmospheric residual oil (>340°C) (Kabe *et. al.*, 1999)

Property	China		Middle East		Middle South America	
	Sheng Li	Da Qing	Arabian Light	Arabian Heavy	Maya	Ithmus
Yields (vol. %)	73.29	70.49	44.71	53.76	60.63	43.23
Specific gravity (15/4 °C)	0.942	0.897	0.9538	0.9855	1.0035	0.9594
Viscosity (cst 60 °C)	n.a	96	103	1020	14000	247
Sulphur (wt %)	1.226	0.1148	3.059	4.274	4.5192	2.6314
Nitrogen (wt %)	n.a	0.2187	0.1749	0.2512	0.5311	0.3385
Vanadium (wt ppm)	3.29	0	27.17	96.67	462.67	102.27
Nickel (wt ppm)	20.63	5.45	6.72	27.75	77	19.36
Canradson Carbon (wt%)	8.6	4.2	7.8	13.3	15.8	9
Asphaltene (wt %)	1.16	0.13	2	9.7	8.5	1.92

Table 2.2 Properties of typical vacuum residual oil (>560 °C) (Kabe *et. al.*, 1999)

Property	China		Middle East		Middle South America	
	Sheng Li	Da Qing	Arabian Light	Arabian Heavy	Maya	Ithmus
Yields (vol. %)	36.51	31.1	14.97	25	36.43	14.94
Specific gravity (15/4 °C)	0.9881	0.9378	1.0217	1.0505	1.0512	1.0312
Viscosity (cst 60 °C)	n.a	1.81 x10 ³	3.33 x10 ⁴	3.9 x10 ⁶	2.57 x10 ⁹	2.82
Sulphur (wt %)	1.66	0.16	4.165	5.63	5.4	3.828
Nitrogen (wt %)	n.a	0.4	0.34	0.425	0.761	0.6683
Vanadium (wt ppm)	41.98	0	75.62	194.2	735	274
Nickel (wt ppm)	6.33	11.82	18.64	55.72	122	52
Canradson Carbon (wt %)	16.4	9	16.5	23.7	25.2	23.6
Asphaltene (wt %)	2.62	0.21	5.2	19.6	15.77	5.23

Table 2.3 Typical elemental composition and H/C atomic ratio of typical petroleum residual oil (Gray, 1994; Kabe *et. al.*, 1999)

Component	Content
Sulphur, wt %	2-7
Nitrogen, wt %	0.2-0.7
Oxygen, wt %	≈ 1
Vanadium, ppm	100-1000
Nickel, ppm	20-200
H/C atomic ratio	1.5-1.9

Table 2.4 Chemical composition of petroleum residual oil (Gray, 1994)


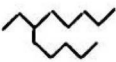

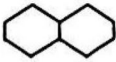

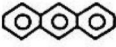
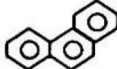
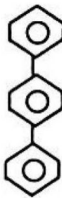
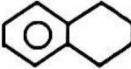
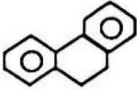

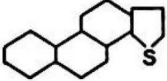



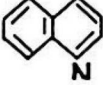
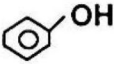
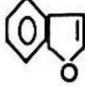
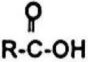
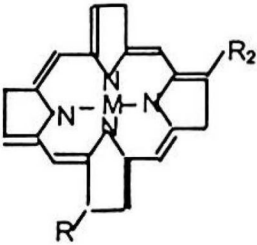
Hydrocarbon Components	Examples
<p>Paraffins</p> <ul style="list-style-type: none"> Saturated straight-chain hydrocarbons that may be presented with the formula C_nH_{2n+1}. 	<p>Isoprenoid </p> <p>T-branched </p>
<p>Naphthenes (cycloparaffins)</p> <ul style="list-style-type: none"> Ring structure saturated hydrocarbons with contain the general formula C_nH_{2n}. Many contain two of more rings fused together. 	<p>Cyclohexane </p> <p>Decalin </p> <p>dimethylcyclopentane </p>
<p>Aromatic structure</p> <ul style="list-style-type: none"> Based on benzene rings, normally substituted with alkyl groups, or bridges to other aromatics. Can be built over promotion of acidic catalysts. 	<p>Anthracene </p> <p>Phenanthrene </p> <p>Terphenyl </p>
<p>Hydroaromatics (naphthenoaromatic)</p> <ul style="list-style-type: none"> Appear in natural oil, as well as in streams that have been hydrogenated. Likely derived from hydrotreated naphthalene rings. 	<p>Tetralin </p> <p>9,10-Dihydrophenanthrene </p>

Table 2.4, continued

Nonhydrocarbon components	Examples
<p>Sulphur</p> <ul style="list-style-type: none"> As thiophene homologs are resistant to further processing, and as sulphides are easily removed. 	<p>Thiophene </p> <p>Sulphides </p> <p>Mercaptans R-SH</p> <p>dibenzothiophene </p>
<p>Nitrogen compounds</p> <ul style="list-style-type: none"> Appear as nonbasic derivatives of pyrrole and basic derivatives pyridine. Highly resistant to removal. 	<p>Pyrrole </p> <p>Pyridine </p> <p>quinoline </p>
<p>Oxygen compounds</p> <ul style="list-style-type: none"> Present as derivatives of furan, ketone, ethers, anhydrides and polar functional groups. 	<p>Phenol </p> <p>Benzofuran </p> <p>Carboxylic acid </p>
<p>Metallic constituents</p> <ul style="list-style-type: none"> Appear as porphyrin metals, which are chelated in porphyrin structures, and also nonporphyrin metals associated with the polar groups of asphaltenes. 	<p>Petroporphyrin </p> <p>Non-porphyrin</p>

These high viscosity and density can be attributed to the high molecular weight compounds. Viscosity data are also used to indicate what thermal forces will be necessary to move petroleum and products around refinery, so reducing viscosity (visbreaking) is important (Gray, 1994).

2.2 HYDROCRACKING AND HYDROTREATING OF RESIDUAL OIL

2.2.1 Hydrocracking process

Hydrocracking is a process for converting large molecules into more valuable smaller molecules in presence of hydrogen that can be used in transportation fuels. Cracking is the process, which produces lighter oils by breaking down heavy oil molecules in presence or absence of hydrogen. This process increases the yield of gasoline from crude oil.

Thermal cracking is the breaking up of heavy oil molecules into lighter fractions by the use of high temperature without the aid of catalyst. Thermal cracking processes are commonly used to convert petroleum residual oil into distillable products, although thermal cracking processes as used in the early refineries are no longer in used and the modern thermal cracking processes is visbreaking (Speight, 1998). The objective of visbreaking is to reduce the viscosity of heavy feedstock and to increase the hydrogen-carbon atomic ratio (H/C atomic ratio). The reduction in viscosity of the unconverted residue tends to reach a limiting value with conversion, although the total product viscosity can continue to decrease (Gray, 1994). Conversion of residue in visbreaking follows first order reaction kinetics. The high viscosity of the residues is thought to be

due to entanglement of the high molecular weight compounds and formation of order structures in the liquid phase. Thermal cracking at low conversion can remove side chains from the asphaltenes and break bridging aliphatic linkages. A 5-10 % conversion of atmospheric residual oil to naphtha is sufficient to reduce the entanglements and structures in the liquid phase and give at least a five fold reduction in viscosity (Speight, 1998).

Martinez *et al.*, (1997) reported interesting experimental results on thermal cracking. They used a batch reactor to carry out the thermal cracking of asphaltenic residue from synthetic crude obtained by coal liquefaction. A second-order reaction was suggested for asphaltene cracking at temperature 425, 435 and 450 °C. The amount of asphaltene and yields of products, oil, gas and coke were presented as a function of residence time.

Wang and Anthony (2003) studied the thermal cracking of asphaltenes by reexamining data obtained by Martinez *et al.*, (1997). They derived the concentration and conversion or residence time relation for the yields involving the secondary cracking of oil, by direct integration of the rate equations. The developed relationship between the coke yield and conversion would make the predications much easier. They reported that thermal cracking of asphaltenes occurs in important heavy-oil upgrading processes such as coking and visbreaking. Their analyses confirmed that at lower temperatures the three-lump model which considered parallel reactions of oil, gas and coke formation described the cracking behaviour whereas at higher temperature the secondary cracking of oil may be considered. This development has the potential to be useful in describing thermal-cracking processes for heavy oils.

Catalytic hydrocracking is the process of breaking up heavier hydrocarbon molecules into lighter hydrocarbon fractions by using heat and catalysts in the presence of hydrogen (Hatch and Mater, 1982). Hydrocracking is an endothermic reaction, provides olefins and other unsaturates for hydrogenation, while hydrogenation, an exothermic reaction, provides heat for cracking (Al-Adwani and Anthony, 1996). Catalytic hydrocracking of residual oil became one of the most important refining processes after it was first commercialized in 1936 by Eugene Houdry. Over the last sixty years, continues efforts to improve catalysts and process technology had lead to the conversion of a larger portion of heavy oils to light and more valuable products (Heinrich *et al.*, 1997).

Catalytic hydrocracking offers several advantages over thermal cracking such as (Gary and Handwerk, 1984):

- Higher gasoline yield.
- Better gasoline octane quality.
- Improved balance of gasoline and distillate production.
- Higher yield of isobutene in the butane fraction.

After distillation of crude oil, most of the heterogeneous compounds particularly sulphur compounds remain in the residue, so hydrotreating processes are taken place during the hydrocracking. Hydrotreating processes (hydrodesulphurization (HDS) and hydrodenitrogenation (HDN)) are catalytic cracking which use hydrogen at high pressure and temperature in the presence a catalyst to reduce heterogeneous compounds (sulphur and nitrogen) and produce lighter oils by cracking the heavy oil molecules. HDS reactions are well known to proceed via two parallel path ways, the hydrogenation

and the direct desulphurization routes (Farag *et al.*, 2003). Conventional supported molybdenum or tungsten sulphide catalysts have generally higher HDS activity relative to HDN activity, and most of the catalysts gave HDN/HDS ratios < 1 (Escalona *et al.*, 2002).

Many investigators have reported the production of light fuels from cracking of heavy oils and removing the undesirable compounds over different cracking catalysts (Tian *et al.*, 1998; Chen and Tsia, 1999; Kaluza and Zdrzil, 2001; Escalona *et al.*, 2002; Farag *et al.*, 2003; Martinez *et al.*, 2003). Tian *et al.*, (1998) carried out the hydrogenation of residual oil in the presence of dispersed water-soluble Ni-Mo catalyst and alumina supported Co-Mo catalyst for comparison of their hydrotreating activities using a 300 ml high pressure batch reactor. The experiments were done under hydrogen pressure of 7 MPa, temperature of 340 °C and time 30, 120 and 240 min. The sample and catalyst loading were 45 g and 0.3 wt%, respectively. Their results revealed that presulphidation treatment of the supported Co-Mo catalyst was important step. Reaction time was important for HDS and HDN activities carried out in batch reactor, affecting the reaction severity. Pretreated catalysts showing gradual changes in removal rate are more active at longer reaction time. The effect of presulphided catalyst was steeper than with reduced catalyst which indicated that better conversion could be achieved by increasing the reaction time at a constant temperature. The results for HDS and HDN activities are shown in Figures 2.2 and 2.3, respectively.

Chen and Tsia (1999) carried out hydrotreating of Kuwaiti atmospheric tower bottom (ATB) residual oil in a stainless steel concurrent down flow trickle bed reactor using a series of aluminum borates (AB) with various Al/B ratios as the support for CoMo and

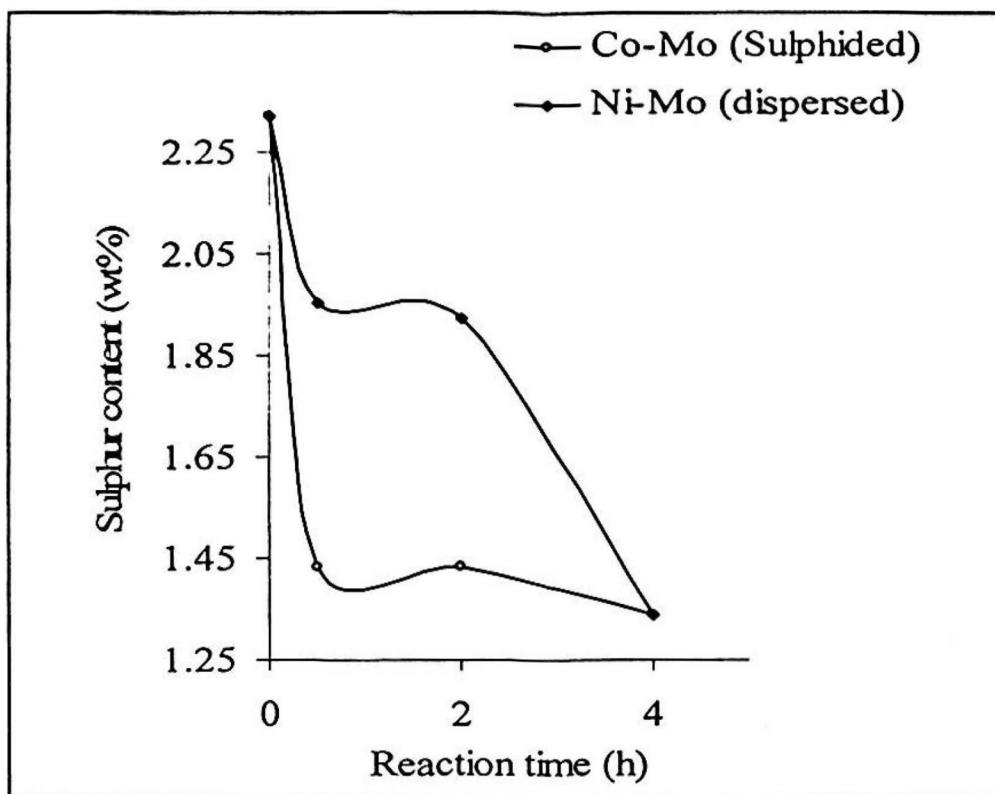


Figure 2.2 HDS activity of dispersed and presulphided supported catalyst (Tian *et al.*, 1998)

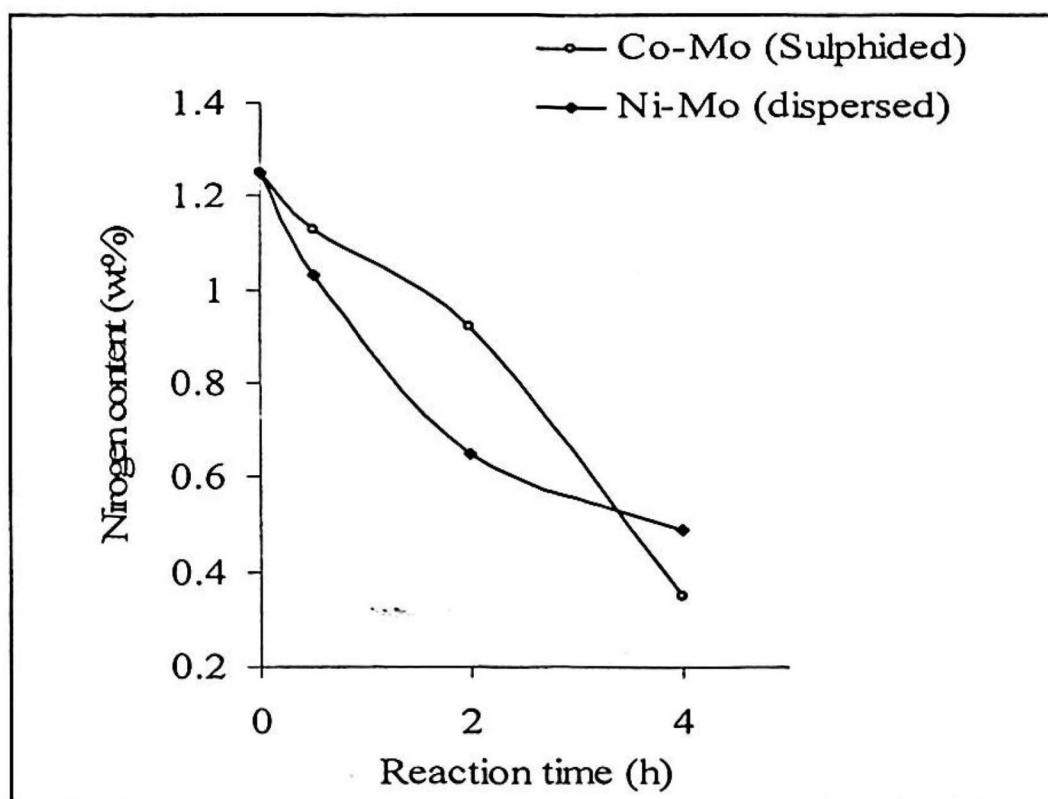


Figure 2.3 HDN activity of dispersed and presulphided supported catalyst (Tian *et al.*, 1998)

NiMo catalysts. The feed was conducted at 663 K, 7.6 MPa, and weight hourly space velocities (WHSV) = 1.5 and the hydrogen flow rate was 300 ml/min. Their results revealed that the AB supported CoMo and NiMo catalysts were more active than those of Al₂O₃-supported ones. This can be rationalized by the presence of boron. Several concurrent effects in AB-supported catalysts may facilitate their hydrotreating activities: enhance the dispersion of active sulphide phase; increase the hydrogenation ability and the amount of active site. All are beneficial for hydrotreating process.

Kaluza and zdrazil (2001) prepared MoO₃ activated carbon catalysts using four different commercial carbon supports derived from natural non-polymeric precursors and carbon black manufactured from heavy petroleum residues. These catalysts were used for hydrodesulphurization process of thiophene in the gas phase in a fixed bed flow reactor at total pressure of 1 MPa and temperature range of 250-400 °C. They found that the adsorption of molybdenum from slurry of MoO₃ in water is a very clean and simple method for the preparation of MoO₃/carbon catalysts. It was concluded that molybdenum trioxide is chemisorbed in a highly dispersed "monolayer" form up to loading of about 15% MoO₃ and then almost levelled off. A strong synergistic effect in activity was achieved by addition of cobalt to the 15% MoO₃/carbon catalyst. They also found that carbon supported catalysts were much more active than their aluminium-supported counterparts. The high surface area of activated carbons is not the main reason for this high activity because the surface area of carbon supported catalysts evaluated by a modified BET method is and not much higher than the surface area of alumina supported catalysts. The specific ability of activated carbon to promote the HDS activity of the deposited sulphide phase has recently been interpreted as a 'sink effect'. This effect is connected with the presence of micropores that 'sink' the excess

of sulphur from the sulphide phase, regenerating sulphur vacancies needed for the HDS reaction.

Escalona *et al.*, (2002) studied the effect of rhenate (Re) loading on the structure activity and selectivity of Re/activated carbon catalysts in HDS and HDN of gas oil. They prepared a series of Re containing catalysts supported on activated carbon (BET surface area of 817 m²/g, total pore volume of 0.637 cm³/g and particle size of 20-26 mesh), with Re loading between 0.74 and 11.44 wt% Re₂O₇. The performance of the catalysts was determined in a high pressure continuous flow microreactor in the temperature range of 325-375 °C under standard conditions: 3 MPa total pressure, 9 h⁻¹ liquid hourly space velocities (LHSV), 3600 h⁻¹ gas hourly space velocities (GHSV), and H₂/feed ratio of 400. They reported that at Re loading below 0.2 atoms nm⁻², Re(x)/AC catalysts had higher HDS activity per gram of catalyst and also per metal atom than equivalent Re(x)/γ-Al₂O₃. The behaviour of intrinsic HDN activity showed similar trends as those observed for HDS activity but with more pronounced differences and up to Re loadings of about 0.4 atomic nm⁻². The Re(x)/AC catalysts were about twice as selective for HDN than Re(x)/γ-Al₂O₃ catalysts over the whole range of metal loading and reaction temperature studied. The increase in HDN selectivity of Re sulphide deposited on carbon compared to on alumina suggests that the carbon support causes a small additional effect on selectivity towards the HDN reaction. The support might introduce structural and textural modifications of the active phase which more favourable to HDN than HDS. The morphology of MoS₂ on activated carbon due to its high dispersion and high fraction of corner sites, leads to high hydrogenation activities. This higher hydrogenation activity of activated carbon supported catalysts compared with the corresponding alumina supported ones could explain the increased HDN/HDS

selectivity. The activated carbon could also take part directly in some of the reaction steps, for instance, its surface oxygenated acidic groups participating in the cleavage of the C-N bond. Another possibility is that the increased HDN selectivity on activated carbon supported catalysts could stem from the formation of a surface Re carbide layer, since metal carbides have shown to be highly active for HDN reactions.

Farag *et al.*, (2003) studied the effect of H₂S as promoter and inhibitor for HDS of dibenzothiophene (DBT) using batch microautoclave reactor. The reactor charged with 0.1–0.2 g catalyst and 10 g, 1 wt % DBT in decane and HDS reaction runs were adjusted to perform at a fixed conditions of 340 °C and 3 MPa H₂. They reported that H₂S creates new active sites some of them maybe excluded from the contribution in the hydrogenation reaction most probably due to the steric geometry hindrance factor. In addition, they suggested that the morphology nature of the created active sites by H₂S, and not the chemical nature that rule the precise control of their contribution on HDS reaction. Finally, they proposed mechanism for H₂S effect. This proposed scheme is depicted in Figure 2.4. The attacking of H₂S molecule in order to fill up the coordinately unsaturated sites will create new sites that are mainly from the geometry point of view can proceed hydrogenation. Reasonably, not all the newly created sites are catalytically active, the only sites which locate to fit the adsorption requirement of the substrate probably at the edges of the MoS₂ phase, is suggested to be usable. The dissociation of hydrogen may lead to -SH and =SH₂ groups. The =SH₂ group is supposed to forward hydrogenation while -SH may help doing direct desulphurization and in some circumstances hydrogenation in which the location geometry of the substrate is a concerned factor. The identity of the active sites and their overall number of them are to be considered factors in the activity promotion.

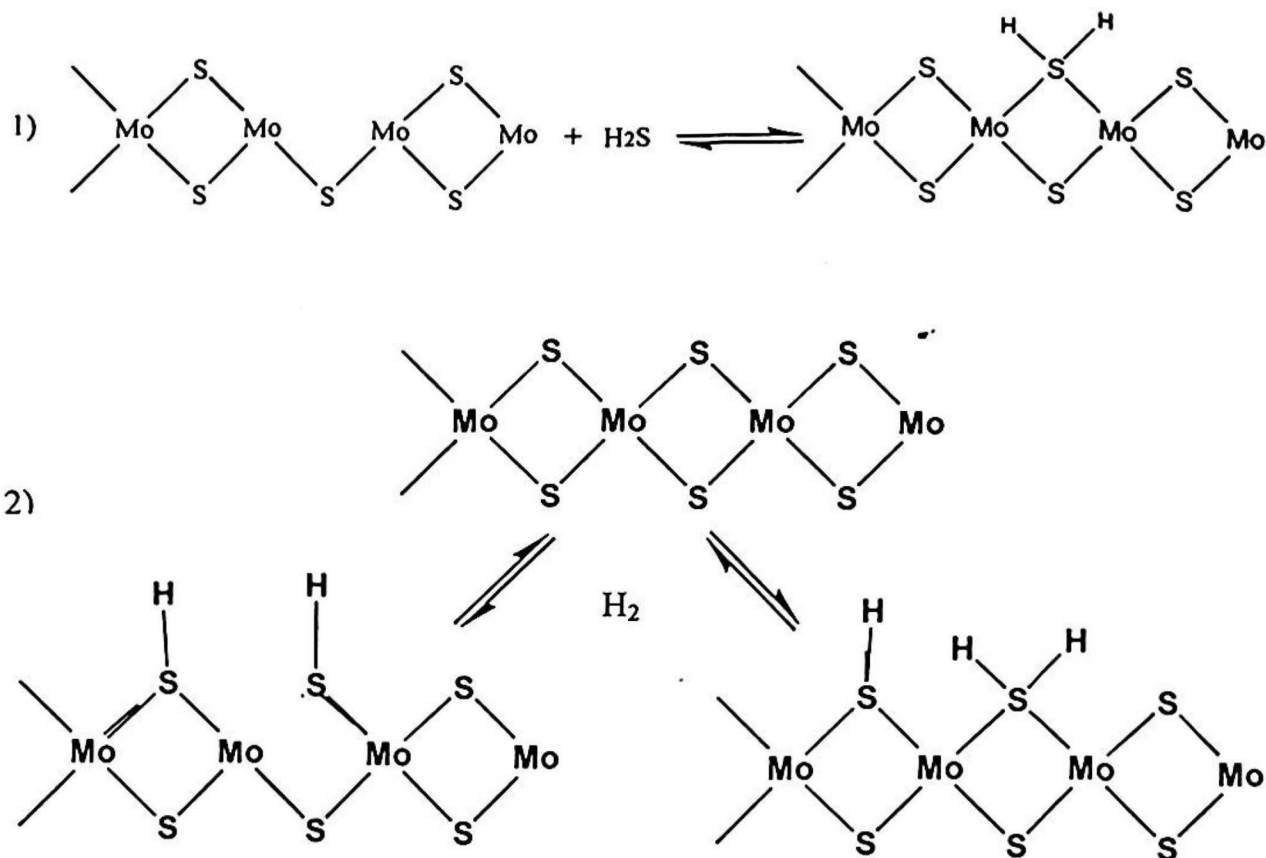


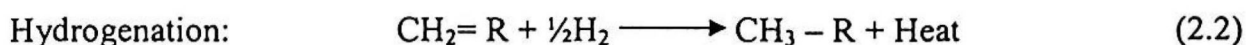
Figure 2.4 Proposed reaction mechanism for the effect of H₂S on HDS reactions (Farg *et al.*, 2003)

Martinez *et al.*, (2003) studied the HDS reaction of heavy vacuum gas oil (HVGO) in a batch reactor, under the following operation conditions: T = 350 °C; P_{H₂} (initial) = 80 kg/cm² and P_{H₂} (final) = 120Kg/cm²; stirring mechanically at 210 rpm; reaction time equal to 3 h. The catalytic study was performed on the Al- and Ti-PILCS (pillared interlayered clays) prepared by means of the alternate microwave irradiation methods loaded with Co and Mo and compared with CoMo/γ-Al₂O₃ and conventional CoMo/PILCS under similar conditions. They found that the evaluation of the catalytic properties of CoMo/Ti-PILCS prepared by means of the microwave radiation methods indicates a HDS activity at least comparable but sometimes superior than their conventional counterparts, in particular when compared with respect to the reference, i.e

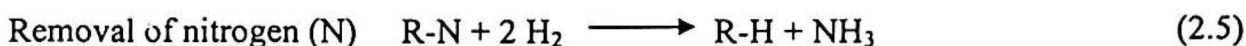
CoMo/ γ -Al₂O₃. The microwave radiation method might induce structural and textural variations on the Al- and Ti-PILCS solids, which in turn might enhance useful catalytic properties of CoMo/Al-, Ti-PILCS for the HDS of Maya crude HVGO.

2.2.2 Chemical reactions

Hydrocracking is hydrogen consuming reaction. Although hundreds of simultaneous reactions are taking place, the chemical fundamentals of this process are well understood. Hydrocracking involves catalytic cracking with hydrogenation forced to prevail by extremely high hydrogen to oil ratio (≈ 1000). Catalytic cracking is the scission of a carbon-carbon single bond while hydrogenation is the addition of hydrogen to a carbon-carbon double bond (Gary, 1984). The role of hydrogen and temperature is very important. All reactions involve hydrogen contact with the reactants at a pressure above 7 MPa and temperature up to 470 °C (Speight, 1998). The feedstock is thermally cracked and hydrogenated to yield products with increased H/C atomic ratio, reduced sulphur and nitrogen content. An increase in the reaction temperature results in an increase in reaction rate but has no significant effect on the conversion. The main types of reactions that take place are:



Hydrotraeting:



These chemical equations are simplified since sulphur, oxygen, nitrogen and metals are present in large heteroatom cyclic compounds. Also taking place in hydrocracking processes are isomerization reactions of straight paraffinic chains to high octane isoparaffins and conversion of aromatic compounds to cycloparaffins (Laine and Trimm 1982). Hydrocracking and hydrotreating are all first-order reactions with hydrocracking as the rate-controlling step, and kinetic data of the reaction follow a Langmuir-Hinshellwood approach (Choudhary and Saraf 1975).

2.2.3 Catalysts

A Catalyst is a substance that increases the rate at which a chemical reaction approaches equilibrium without itself becoming permanently involved in the reaction. The main processes that use catalysts for petroleum residual oil upgrading are: hydrotreating, hydrocracking and fluid catalytic cracking (FCC). The improvements made in petroleum residual oil conversion catalysts over the last 15 years are shown in Table 2.5 (Absi-Halabi *et al.*, 1997).

Hydrocracking process needs dual function catalysts, hydrogenation and cracking functions. Active component and promoters sulphides provide hydrogenation function. These active compositions saturate aromatics in the feed, saturate olefins formed in the cracking, and protect the catalyst from poisoning by the coke. Supports provide the cracking functions, where the cracking takes place on strong acid sites in the supports.

Most of the catalysts have three types of easily distinguishable components, these are (Richardson, 1989):

A- Active components